A New Method for Atmospheric Correction and Aerosol Optical Property Retrieval for VIS-SWIR Multi- and Hyperspectral Imaging Sensors: QUAC (QUick Atmospheric Correction)

L. S. Bernstein, S. M. Adler-Golden,
R. L. Sundberg, R. Y. Levine, T. C. Perkins, and A. Berk
Spectral Sciences, Inc.
4 Fourth Avenue
Burlington, MA 01803-3304

A. J. Ratkowski, G. Felde and M. L. Hoke
Air Force Research Laboratory
29 Randolph Road
Hanscom AFB, MA 01731-3010

***Abstract*-We describe a new VNIR-SWIR atmospheric correction method for multi- and hyperspectral imagery, dubbed QUAC (QUick Atmospheric Correction) that also enables retrieval of the wavelength-dependent optical depth of the aerosol or haze and molecular absorbers. It determines the atmospheric compensation parameters directly from the information contained within the scene using the observed pixel spectra. The approach is based on the empirical finding that the spectral standard deviation of a collection of diverse material spectra, such as the endmember spectra in a scene, is essentially spectrally flat. It allows the retrieval of reasonably accurate reflectance spectra even when the sensor does not have a proper radiometric or wavelength calibration, or when the solar illumination intensity is unknown. The computational speed of the atmospheric correction method is significantly faster than for the first-principles methods, making it potentially suitable for real-time applications. The aerosol optical depth retrieval method, unlike most prior methods, does not require the presence of dark pixels. In this paper, QUAC is applied to atmospherically correction several AVIRIS data sets. Comparisons to the physics-based FLAASH code are also presented.**

I. INTRODUCTION

A critical first step in the analysis of visible through short-wavelength infrared (SWIR) hyperspectral or multispectral imagery (HSI or MSI) is atmospheric correction or compensation, in which atmospheric absorption and scattering effects are removed and the data are reduced to surface spectral reflectance (see Fig. 1). A number of atmospheric-correction methods and algorithms exist, including algorithms based on first-principles radiation transport calculations [1-10], and empirical approaches such as the Empirical Line Method (ELM) [11,12], which relies on two or more known reflectances in the image. However, none of these methods provides the ideal combination of high accuracy, high computational speed and independence from the need for prior knowledge.

This paper focuses on validation of a new, semi-empirical atmospheric-correction method, dubbed QUAC, which also enables retrieval of the wavelength-dependent optical depth of aerosol or haze and molecular absorbers. A more detailed description of the QUAC approach was recently presented at the 2004 AVIRIS Workshop [13] and it is only summarized here. It allows the retrieval of approximate reflectance spectra even when the sensor does not have a proper radiometric or wavelength calibration, or when the solar illumination intensity is unknown, such as when a cloud deck is present. Computational speed is much faster than for the first-principles methods, making it potentially suitable for real-time applications. In tests to date, QUAC has yielded remarkably good agreement with a state-of-the-art first-principles algorithm. Like the ELM, QUAC assumes a linear relationship between spectral reflectance and measured radiance, a good approximation for most scenes.

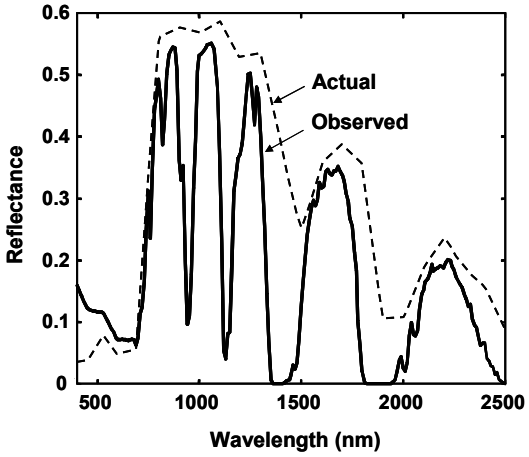

Figure 1. MODTRAN calculation of the apparent reflectance of a vegetation pixel as observed from space with nadir viewing, a Mid-Latitude Summer model atmosphere, and a Rural aerosol with visibility=23km.

The standard radiance equation may be written as

$$\rho_j(\lambda) = A(\lambda) + \frac{B(\lambda)}{1 - S(\lambda) < \rho(\lambda) >} \rho_j^o(\lambda) + \frac{C(\lambda)}{1 - S(\lambda) < \rho(\lambda) >} < \rho(\lambda) >, \quad \textbf{(1)}$$

where ρ_j is the observed reflectance (the radiance normalized by the surface normal component of the solar flux) for the j'th pixel at a spectral band centered at wavelength λ, ρ_j^o is the actual surface reflectance, $<\rho>$ is a spatially averaged surface reflectance. A, B, C and S are coefficients that describe the

0-7803-9051-2/05/$20.00 (C) 2005 IEEE

Report Documentation Page

Form Approved
OMB No. 0704-0188

1. REPORT DATE	2. REPORT TYPE	3. DATES COVERED
25 JUL 2005	**N/A**	**-**

4. TITLE AND SUBTITLE
A New Method for Atmospheric Correction and Aerosol Optical Property Retrieval for VIS-SWIR Multi- and Hyperspectral Imaging Sensors: QUAC (QUick Atmospheric Correction)

5a. CONTRACT NUMBER

5b. GRANT NUMBER

5c. PROGRAM ELEMENT NUMBER

6. AUTHOR(S)

5d. PROJECT NUMBER

5e. TASK NUMBER

5f. WORK UNIT NUMBER

7. PERFORMING ORGANIZATION NAME(S) AND ADDRESS(ES)
Spectral Sciences, Inc. 4 Fourth Avenue Burlington, MA 01803-3304

8. PERFORMING ORGANIZATION REPORT NUMBER

9. SPONSORING/MONITORING AGENCY NAME(S) AND ADDRESS(ES)

10. SPONSOR/MONITOR'S ACRONYM(S)

11. SPONSOR/MONITOR'S REPORT NUMBER(S)

12. DISTRIBUTION/AVAILABILITY STATEMENT
Approved for public release, distribution unlimited

13. SUPPLEMENTARY NOTES
See also ADM001850, 2005 IEEE International Geoscience and Remote Sensing Symposium Proceedings (25th) (IGARSS 2005) Held in Seoul, Korea on 25-29 July 2005. , The original document contains color images.

14. ABSTRACT

15. SUBJECT TERMS

16. SECURITY CLASSIFICATION OF:			17. LIMITATION OF ABSTRACT	18. NUMBER OF PAGES	19a. NAME OF RESPONSIBLE PERSON
a. REPORT	b. ABSTRACT	c. THIS PAGE			
unclassified	**unclassified**	**unclassified**	**UU**	**4**	

Standard Form 298 (Rev. 8-98)
Prescribed by ANSI Std Z39-18

transmission and scattering effects of the atmosphere. Their physical origin is highlighted in Figure 2. The first coefficient, A, accounts for light that never encounters the surface, but is scattered and absorbed within the atmosphere. The second, B, accounts for the Sun-surface-sensor path direct transmittance. The third, C, accounts for diffuse transmittance and gives rise to the "adjacency effect," a spatial blending induced by atmospheric scattering. The length scale of the adjacency effect is typically of order ~0.5km, thus $<\rho>$ is typically a slowly varying function of position within a large image. S, the atmospheric spherical albedo, accounts for enhancement of the ground illumination by atmospheric reflection.

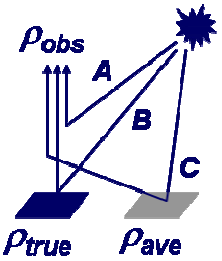

Figure 2 . Radiation-transfer contributions to the observed apparent reflectance, ρ_{obs}.

Eq. (1) reduces to a linear form under many common conditions in which: (1) $S<\rho>$ is small and when either (2) the diffuse and direct transmittance terms can be combined with a single reflectance variable, or (3) the diffuse term can be combined with the backscattering term. Situation (1) occurs frequently, when the visibility is reasonably high or when the ground is dark in the visible (such as with vegetation, water or dark soil). Situation (2) occurs when the pixels are very large, several hundred meters in size. Situation (3) occurs when the scene materials are fairly uniformly interspersed or when the image covers a small geographic area (< ~1 km), making $<\rho>$ nearly constant, or when the visibility is high, making the diffuse transmittance term small. When (1) and (3) apply, Eq. (1) reduces to the linear equation

$$\rho_j(\lambda) = A(\lambda) + B(\lambda)\rho_j^o(\lambda) + C(\lambda) < \rho(\lambda) > . \qquad \textbf{(2)}$$

With the linear Eq. (2), the aim of atmospheric compensation is essentially the determination of an offset, $A+C<\rho>$, and gain parameter, B, in order to retrieve the surface reflectance, ρ_j^o. Numerous approaches to this problem have been developed. The ELM assumes that the radiance image contains some pixels of known reflectance. This method is not generally applicable, as in-scene known reflectances are often not available.

First-principles methods express the Eq. (1) or Eq. (2) parameters in terms of atmospheric physical variables, such as column water vapor and aerosol optical depth or visibility. For retrieving optical depth, methods are available that rely on modeling the aerosol backscatter over "dark" pixels such as vegetation and dark soil [14] or water bodies. However, difficulties in determining the optical depth arise when there is a lack of suitable dark pixels in the scene, or when the sensor is at a low altitude, within the aerosol layer, so that the backscatter it measures is a small (and generally unknown) fraction of the total.

Like many first-principles methods, QUAC determines the atmospheric compensation parameters directly from the information contained within the scene (observed pixel spectra), without ancillary information. However, unlike most other methods, its aerosol optical depth retrieval approach does not require the presence of dark pixels. The retrieved optical depth information can therefore be utilized to improve the accuracy of methods that use first-principles modeling. In particular, it can be used to set the optical depth of a model aerosol when dark pixels are unavailable, or to select from among alternative model aerosols to provide consistency with optical depths retrieved from a dark-pixel method.

II. QUAC ALGORITHM DESCRIPTION

The underlying assumptions of the approach are:

- There are a number (≈10 or more) of diverse pixel spectra (diverse materials) in a scene,
- The spectral standard deviation of ρ_j^o for a collection of diverse materials is a nearly wavelength-independent constant, and an additional, helpful, assumption is that,
- There are sufficiently dark pixels ($\rho_j^o(\lambda)\approx 0$) in a scene to allow for a good estimation of the nearly spatially invariant baseline contribution, $\rho_b = A + C<\rho>$.

The first assumption is usually applicable, as it only requires that a handful of pixels out of typically ~10^5 to 10^6 pixels display diverse spectra. The most notable exception would be a scene over completely open and deep water, in which case the material reflectance is well known *a priori*. The diverse spectra can be selected using any of a number of spectral diversity metrics and algorithms, such as endmembers. The second assumption appears to be generally true based on our empirical observation, and is likely related to the lack of spectral correlation between diverse materials. The third assumption is frequently applicable, as most scenes will contain a number of very dark pixels from such surfaces as water bodies, vegetation and cast shadows. For the atypical cases that violate this assumption, there are alternative methods [13] for estimating a reasonable baseline. The atmospheric correction step just involves re-arranging Eq. (2) to solve for $\rho_j^o(\lambda)$ given B and the baseline. A key attribute of QUAC is its applicability to any sensor viewing or solar elevation angle.

Under the above-stated assumptions, the spectral standard deviation of Eq. (2) for a set of diverse pixel spectral can be expressed as

$$\sigma\rho(\lambda) = B(\lambda)\sigma\rho^o(\lambda) . \qquad \textbf{(3)}$$

For reasons mentioned earlier, $A + C<\rho>$ can be taken as a constant in many, if not most, cases, so it makes no contribution to the standard deviation. In cases where it varies

significantly within the scene, the image can be divided into smaller pieces, as discussed below. Since $\sigma\rho^{o}$ is assumed to be spectrally invariant, then, to within a normalization factor designated g_o, $\sigma\rho$ represents the correction factor, B. The actual surface spectral reflectance can be retrieved using the extracted in-scene-determined compensation parameters and re-arranging Eq. (2) to yield

$$\rho_j^o(\lambda) = \frac{\rho_j(\lambda) - \rho_b(\lambda)}{g_o \sigma\rho(\lambda)}, \quad \textbf{(4)}$$

where $\rho_b = A + C\langle\rho\rangle$ is the baseline contribution. It is noted that the $B(\lambda)$ is a direct measure of the wavelength-dependent aerosol extinction and can be used to retrieve the aerosol optical properties. The approach for doing this was previously described [13]. Our focus here is on the application of QUAC to atmospheric correction.

III. VALIDATION USING REAL AND SIMULATED IMAGERY

QUAC was evaluated against a wide variety of data consisting of multi- and hyperspectral imagery for different types of scenes, urban and rural, and spanning a wide range of atmospheric conditions. The data are from the airborne hyperspectral AVIRIS sensor (224 spectral channels from ~400 to 2500nm, 2-20m GSD).

QUAC was used to perform atmospheric correction and aerosol property retrieval on two very different AVIRIS data collects. As depicted in Figure 3, one corresponds to high visibility and moderate humidity, and the other to low visibility and high humidity. The NASA Stennis data is particularly useful because the Stennis site contains a large number of ground truth materials/panels (these are visible in the lower left corner of Figure 3).

The first step in the process is the selection of diverse pixel spectra. For this analysis, we used the fast and automated SMACC (Sequential Maximum Angle Convex Cone) [16] endmember code. We used only ten window region wavelengths in order to further speed up finding the endmembers. The results for the NASA Stennis scene are displayed in Figure 4. It is evident that this set spans a wide variety of spectral shapes and reflectance values. Several endmembers are quite dark, and the lowest reflectance value for each channel defines the baseline spectrum.

The next step is to compute the standard deviation of the selected pixels. Before this is done, some refining of the initial selection usually occurs. This involves weeding out spectra with sharp features, mainly vegetation spectra that display a steep rise around 700nm (the chlorophyll red edge). Pixels containing cirrus clouds, which can be easily discerned using established algorithms, are also rejected. The standard deviations for the NASA Stennis and North Carolina SCAR data are presented in Figure 5. The absorption due to the 940nm H_2O band is clearly evident, and the much deeper feature seen in the North Carolina data is indicative of a much higher humidity level. Additional, weaker absorption features, such as the 840nm H_2O and 760nm O_2 bands are easily discernible. The general upper bounding envelope to these curves, formed by spectral regions outside of the absorption features, is a direct measure of the aerosol extinction for the L-shaped path from the Sun to the surface to the sensor (i.e., the B coefficient). By inspection, it is quite obvious that the Stennis scene corresponds to a high visibility while the North Carolina scene displays approximately an order of magnitude more aerosol extinction and hence a much lower visibility.

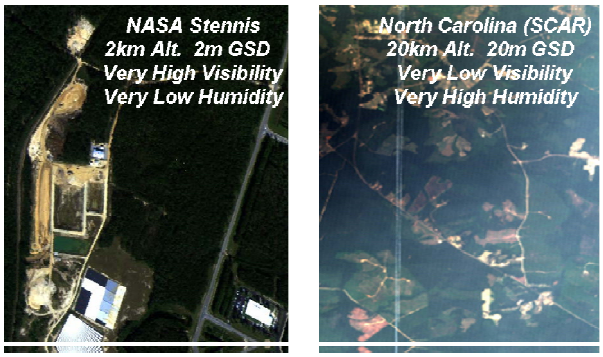

Figure 3. RGB image of the AVIRIS data sets used for evaluation of QUAC.

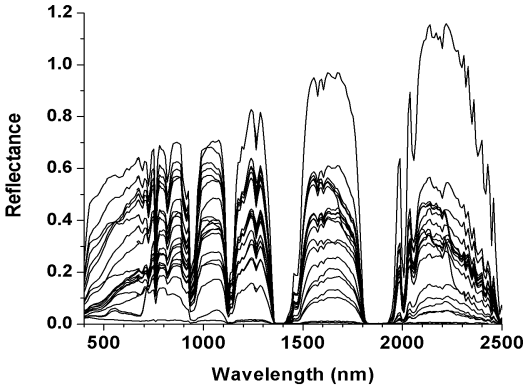

Figure 4. The first twenty endmembers selected by SMACC using the apparent reflectances from the NASA Stennis data.

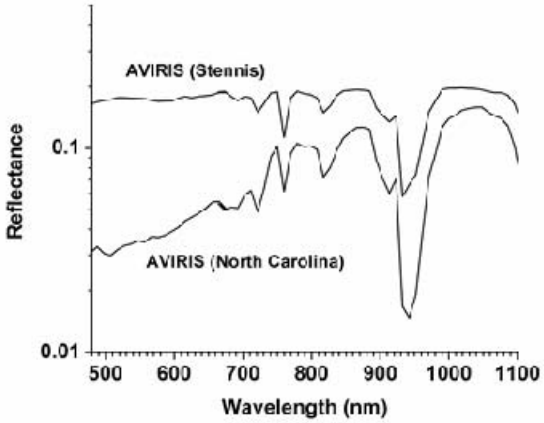

Figure 5. Spectral standard deviations based on the selected endmembers for the Stennis and North Carolina AVIRIS data sets.

From the above information, baseline and standard deviation, the entire data cube can be atmospherically corrected. Sample results for the Stennis data are shown in Figure 6 and include comparisons to FLAASH [7,8] results and ground truth measurements. In this instance, and in general, QUAC compares well to FLAASH. The computational time required for the end-to-end QUAC process for an entire AVIRIS data cube (512x512 pixels and 224 spectral channels is ~1min on a 1.6GHz Pentium IV PC. This is based on relatively slow IDL coding for the endmember selection and atmospheric correction steps. For comparison, FLAASH, which run a series of MODTRAN calculations, requires ~5-10min to perform the atmospheric correction.

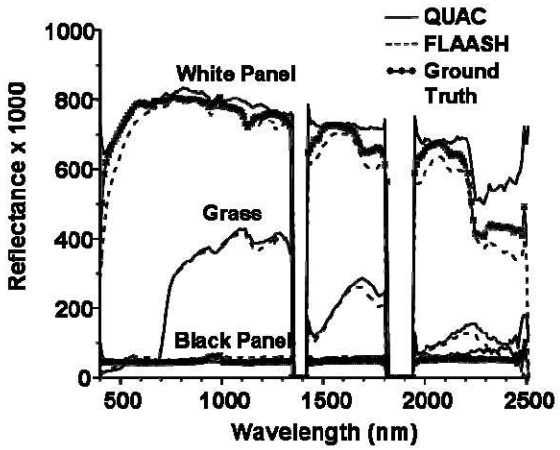

Figure 6. Comparison of QUAC atmospherically-corrected reflectances to those obtained from FLAASH and ground truth measurements for the Stennis data.

IV. CONCLUSIONS AND FUTURE DIRECTIONS

A new semi-empirical algorithm, QUAC, for atmospheric correction and aerosol optical properties retrieval for VNIR-SWIR HSI and MSI sensors has been developed. Initial applications of QUAC to atmospheric correction of HSI AVIRIS and MSI Landsat-7 data [13] and simulated HSI HyMap data [13] show surprisingly good performance, nearly comparable to that of a first-principles physics-based code. Continued development and validation of QUAC is planned using a wider variety of HSI and MSI data sets, including simulated data, and through field measurements involving full characterization of the aerosol column concurrent with airborne and/or satellite-based HSI and MSI observations. Computational speed-ups, automation and, eventually, the development of an on-board data processing capability will also be explored.

ACKNOWLEDGEMENTS

Spectral Sciences, Inc. efforts were funded through an AFRL Phase I SBIR project F19628-02-C-0054 with additional support provided via AFRL F19628-02-C-0078 and Spectral Sciences, Inc. IR&D activity.

REFERENCES

[1] Gao, B.-C. M. J. Montes, Z. Ahmad, and C.O. Davis, "Atmospheric Correction Algorithm for Hyperspectral Remote Sensing of Ocean Color from Space," *Applied Optics,* 39, 887-896, 2000.

[2] Gao, B.-C., K.B. Heidebrecht, and A.F.H. Goetz, "Derivation of Scaled Reflectances from AVIRIS Data," *Proceedings of the Fourth Annual JPL Airborne Geoscience Workshop*, Vol. I. pp.35-36, 1993.

[3] Montes, M.J., B.-C. Gao, and C.O. Davis, "A new algorithm for atmospheric correction of hyperspectral remote sensing data," *SPIE Proceedings, Geo-Spatial Image and Data Exploitation II, Vol. 4383*, pp. 23-30, 2001.

[4] Green, R.O., D.A. Roberts, and J.E. Conel, "Characterization and Compensation of the Atmosphere for Inversion of AVIRIS Calibrated Radiance to Apparent Surface Reflectance," *Summaries of the Sixth Annual JPL Earth Science Workshop*, JPL Publication 96-4, Vol. 1, pp. 135-146, 1996.

[5] Miller, C. J., "Performance assessment of ACORN atmospheric correction algorithm," *SPIE Proceedings, Algorithms and Technologies for Multispectral, Hyperspectral, and Ultraspectral Imagery VIII*, 4725, pp. 438-449, 2002.

[6] Adler-Golden, S.M., M.W. Matthew, L.S. Bernstein, R.Y. Levine, A. Berk, S.C. Richtsmeier, P.K. Acharya, Anderson, G.P., G. Felde, J. Gardner, M. Hoke, L.S. Jeong, B. Pukall, J. Mello, A. Ratkowski and H.-H. Burke, "Atmospheric Correction for Short-wave Spectral Imagery Based on MODTRAN4," *Summaries of the Eighth Annual JPL Earth Science Workshop*, JPL Publication 99-17, pp. 12-23, Jet Propulsion Laboratory, Pasadena, CA., 1999.

[7] Matthew, M.W., S.M. Adler-Golden, A. Berk, G. Felde, G.P. Anderson, D. Gorodetzky, S. Paswaters and M. Shippert, "Atmospheric Correction of Spectral Imagery: Evaluation of the FLAASH Algorithm with AVIRIS Data," *SPIE Proceeding, Algorithms and Technologies for Multispectral, Hyperspectral, and Ultraspectral Imagery IX*, 5093, pp. 474-482, 2003.

[8] Matthew, M.W., S.M. Adler-Golden, A. Berk, S.C. Richtsmeier, R.Y. Levine, L.S. Bernstein, P.K. Acharya, G.P. Anderson, G.W. Felde, M.P. Hoke, A. Ratkowski, H.-H. Burke, R.D. Kaiser, and D.P. Miller, "Status of Atmospheric Correction Using a MODTRAN4-based Algorithm," *SPIE Proceeding, Algorithms for Multispectral, Hyperspectral, and Ultraspectral Imagery VI*, *4049*, pp. 199-207, 2000.

[9] Qu, Z., A.F.H. Goetz, and B. Kindel, "High-accuracy Atmospheric Correction for Hyperspectral Data (HATCH)," *Proceedings of the Ninth AVIRIS Earth Sciences and Applications Workshop*, JPL Publication 00-18, pp. 373-380, Jet Propulsion Laboratory, Pasadena, CA, 2000.

[10] Richter, R. and D. Schlaepfer, "Geo-atmospheric processing of airborne imaging spectrometry data Part 2: atmospheric/topographic correction" *Int. J. Remote Sensing*, 23, 2631-2649, 2002.

[11] Roberts, D. A., Y. Yamaguchi, and R. J. P. Lyon, "Calibration of Airborne Imaging Spectrometer data to percent reflectance using field spectral measurements," *19th International Symposium on Remote Sensing of Environment*, Ann Arbor, MI, 1985.

[12] Kruse, F. A., K. S. Kierein-Young, and J. W. Boardman, "Mineral mapping at Cuprite, Nevada with a 63-channel imaging spectrometer," *Photogrammetric Engineering & Remote Sensing*, 56, 83-92, 1990.

[13] Bernstein, L. S., S. M. Adler-Golden, R. L. Sundberg, R. Y. Levine, T. C. Perkins, A. Berk, A. J. Ratkowski, and M. L. Hoke, **"**A new method for atmospheric correction and aerosol property retrieval for VIS-SWIR multi- and hyperspectral imaging sensors: QUAC (QUick Atmospheric Correction)," *Proceedings of the 2004 AVIRIS Workshop,* Jet Propulsion Laboratory, Pasadena, CA, 2004.

[14] Kaufman, Y.J., A.E. Wald, L.A. Remer, B.-C. Gao, R.-R. Li and L. Flynn, "The MODIS 2.1-μm Channel-Correlation with Visible Reflectance for Use in Remote Sensing of Aerosol," *IEEE Trans. Geosci. Remote Sens.*, 35, 1286-1298, 1997.

[15] Berk, A., L.S. Bernstein, G.P. Anderson, P.K. Acharya, D.C. Robertson, J.H. Chetwynd and S.M. Adler-Golden, "MODTRAN Cloud and Multiple Scattering Upgrades with Application to AVIRIS," *Remote Sens. Environ,*. 65, 367-375, 1998.

[16] Gruninger, J.H., M.J. Fox and R.L. Sundberg, "Hyperspectral Mixture Analysis using Constrained Projections onto Material Subspaces," *Proceedings of the International Symposium on Spectral Sensing Research,* Québec City, pp. 162-170, 2001.